31st Annual International Conference of the IEEE EMBS
Minneapolis, Minnesota, USA, September 2-6, 2009

Ultrasound Mediated Drug Delivery: The effect of microbubbles on a gel boundary

Charles. F. Caskey, Shengping Qin, Katherine W. Ferrara, *Senior Member, IEEE*

***Abstract*—When microbubble contrast agents are driven by ultrasound, the transport of drugs and particles across cell membranes and blood vessel walls is enhanced. While a wide range of acoustic parameters enhance delivery, the acoustic parameters that maximize delivery while simultaneously minimizing biological effects have not been fully characterized. Here, we use a gel phantom with a Young's modulus similar to that of tissue to directly observe bubble interaction with the gel surface during insonation. Using parameters relevant to diagnostic imaging and drug delivery, we observe fluid jets that impinge on the surface and tunnels that follow the sound beam axis.**

I. Introduction

After the injection of ultrasound contrast agents, insonation of a region of interest causes microbubbles within the vasculature to expand and rapidly collapse. Mathematical models and experimentally-acquired images show that microbubbles oscillating near a boundary create fluid jets capable of disrupting the compliant boundaries [1-3]. Delivery of particles beyond the blood-brain barrier and the delivery of plasmid DNA to the pancreas have each been enhanced by insonifying microbubbles, typically with a low ultrasound frequency [4-8]. Varying the center frequency and intensity of the sound field to reduce the risk of petechial hemorrhage [9] and enhance gadolinium delivery to the brain [10] have each been reported, but the precise mechanism for permeability enhancement and extravascular delivery is not fully understood. Here, we examine microbubble oscillation in compliant vessels to elucidate mechanisms of boundary disruption through tunnel formation.

II. Materials and Methods

Microbubbles in a gel phantom were optically imaged during a long ultrasonic pulse with a transmission frequency of 1 MHz, a pulse repetition frequency (PRF) of 10 Hz and pulse duration (PD) of 10 msec. The PRF and PD were chosen to match parameters frequently used in drug delivery studies and differ from typical imaging pulse sequences, where PRF is in the kilohertz range and PD is on the order of microseconds. The ultrasound system consists of a 1.91-cm-diameter US source, spherically focused at a depth of 5.08 cm and aligned such that the acoustic field and observation area overlap. Acoustic alignment was verified with a needle hydrophone (HNZ-0400; Onda Corp, Sunnyvale, CA), and the transducer was driven by an arbitrary waveform generator (AWG2021; Tektronix, Irvine, CA) and a 55-dB radiofrequency amplifier (3200L; ENI; Rochester). The gel phantom was a small block (30 x 20 x 2 mm) of 0.75% (w/v) OmniPur agarose gel (EM Science, Gibbstown, NJ, USA) with an embedded 230-μm channel. The phantom was created by heating a 0.75% agarose solution to 90 C to make a molten gel and casting into a mold containing a 230-μm channel. Lipid-shelled microbubbles with a formulation similar to Definity® were made in-house using techniques described in [11]. The stock concentration of microbubbles was approximately 1.5 x 10^{10} bubbles / mL, with a mean diameter of 1.7+/-1.6 μm. The stock solution was diluted in distilled water so that the final solution ranged from the dosage used for diagnostic therapy (~1.6 * 10^5 bubbles injected / mL blood) to high dosages used in many drug delivery experiments (~2.5 * 10^7 bubbles injected / mL blood). A perfusion pump was set so that the flow rate within the vessel was approximately 36 mm/sec. After insonation, a solution of blue 500-nm microbeads (Polysciences, Warrington, PA) was injected to assist in delineation of wall boundaries within the gel. Images with long exposure times were captured to show the effects of microbubble oscillation, while high-speed strobe images were acquired to show nanosecond-scale microbubble activity during oscillation. The ability for microbubbles to disrupt the vessel wall was quantified by measuring the width of tunnels formed, as well as the overall area of wall disruption. High-speed images were acquired using a copper vapor strobe-based system, described in [12], capable of capturing single 2D frames with an exposure time of 30 nsec. All image measurements were performed with ImageJ (NIH http://www.nih.gov/).

III. Results

Figure 1a-b contains two sequential images of a cluster of microbubbles during the first moments after the onset of insonation with a peak negative ultrasound pressure of 1.5 MPa. Figure 1b is acquired 0.2 msec after the onset of insonation, and the cluster of bubbles has coalesced into a single, larger microbubble that reaches a diameter of approximately 50 μm during the negative half-cycle of the acoustic pulse. A high speed and high magnification image (Figure 1c) of a bubble insonified with the same acoustic pulse indicates complex interaction between multiple bubbles and surrounding objects to form a fluid jet with a

minimum neck diameter of approximately 4 μm. The bubbles undergo a net displacement in the direction of ultrasound propagation. In a typical experiment, a bubble as shown in Figure 1a-c will interact with the gel wall for the entire duration of the acoustic pulse, generating tunnels with diameters of greater than 40 μm, as shown in Figure 1d (arrows indicate tunnels outside the vessel lumen). The newly-formed tunnels are always directed in the ultrasound propagation direction and only observed on the distal side of the flow channel's wall.

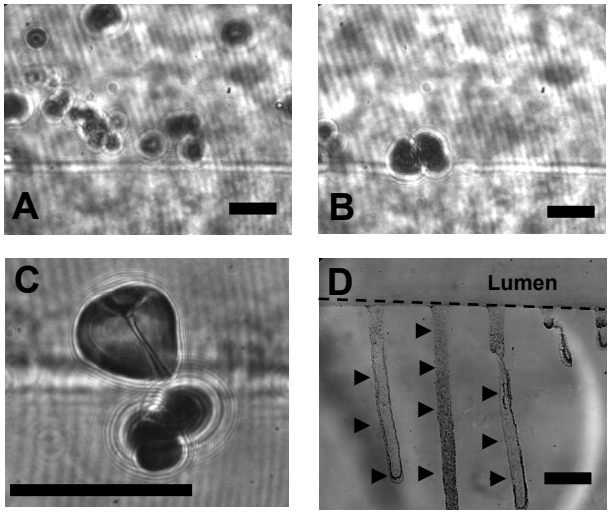

Figure 1. Optical images of microbubble cluster response to 1 MHz ultrasound pulse with a peak negative pressure of 1.5 MPa. (a) The initial cluster of bubbles undergo constrained expansion that is followed by coalescence into a single bubble (shown in (b)) within 10 msec. (c) High magnification image of a liquid jet within a bubble (diagonal line within largest bubble). (d) Post-injection of 500-nm microbeads delineates the disrupted gel area resulting from 200 10 msec pulses. Scale bars are 50 μm. Ultrasound waves propagate from top to bottom in the page plane.

For a 1 MHz acoustic pulse with a PD of 10 msec, tunnel width increases with increasing peak negative ultrasound pressure (Figure 2). The mean tunnel width approaches the maximum predicted expansion of a 9.3-μm diameter bubble oscillating in an infinite fluid [12]. A pressure threshold for tunnel formation exists between 1 and 1.2 MPa.

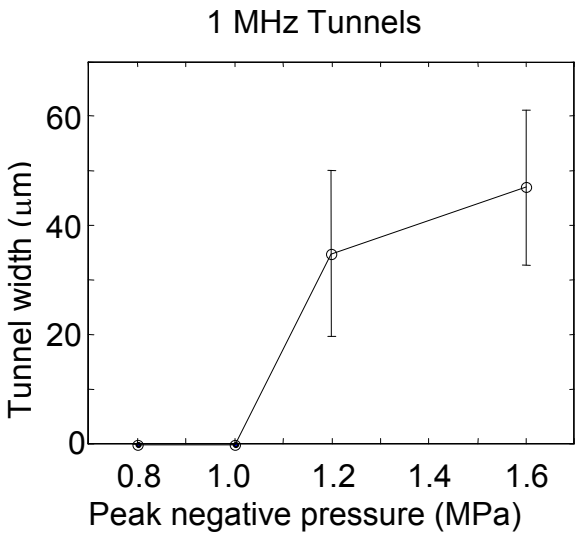

Figure 2. Optical measurements of tunnel width (microns) versus peak negative ultrasound pressure (MPa) following insonation of microbubbles in a small compliant channel using a 1 MHz center frequency.

IV. Discussion

During an acoustic pulse, high concentrations of microbubbles coalesce due to the influence of an attractive force, known as a secondary radiation or Bjerknes force [13, 14]. Simultaneously, the oscillating gas bubbles are displaced in the direction of ultrasound propagation by the primary force of the sound wave [13]. After coalescence and translation toward the gel wall, the newly-formed, larger bubble undergoes many oscillatory cycles during which fluid jets occur, as evidenced by Figure 1c. Repeated oscillation in the same location results in the formation of a small tunnel.

Three mechanisms for tunnel formation are apparent from our observations: fluid jets, radiation force and forces produced by the volumetric expansion of the oscillating bubble. A simplified analysis of the fluid jets indicates that they can generate local pressures in the range of hundreds of megaPascals [12]. This pressure exceeds the tensile strength of the gel and therefore likely plays a role in tunnel formation.

The stress produced by primary radiation force on a large bubble oscillating at very high pressure may also be sufficient to disrupt the gel. Dayton et al. estimates the radiation force on a 1.63 μm bubble as ~1 x 10^{-5} N during a 2.25 MHz acoustic pulse (peak negative pressure of 100 kPa) [13]. The acoustic pulses used in our study have a much higher peak negative pressure, and therefore, the stress due to radiation force could contribute to the disruption of the gel. Once tunnel formation has begun, the large bubble oscillates within a tunnel with a comparable diameter, generating a circumferential stress that may also contribute to the breakdown of the gel [3].

Through a sequence of studies, we have observed that tunnel formation occurs easily with a high concentration and a long acoustic pulse for frequencies as high as 5 MHz. Alternatively, a diagnostic concentration of microbubbles does not produce tunnel formation for frequencies above 2.25 MHz, and short acoustic pulses are less likely to disrupt the gel wall.

V. Conclusion

The studies presented here outline important factors that must be considered in designing safe and effective drug delivery systems. Here, high concentrations of microbubbles coalesced, allowing for the formation of large bubbles capable of disrupting a gel with a Young's modulus on the order of soft tissue. Although the gel phantom differs greatly from living tissue, the study facilitates direct observation of the generation of small pores and tunneling into the gel, which may aid in understanding the mechanism of ultrasound-enhanced drug delivery.

Acknowledgment

The authors would like to acknowledge funding from NIH R01CA103828 and R01CA112356

References

[1] Prentice, P., Cuschieri, A., Dholakia, K., Prausnitz, M., and Campbell, P.: 'Membrane disruption by optically controlled microbubble cavitation', Nat Phys, 2005, 1, (2), pp. 107-110

[2] Kodama, T., and Tomita, Y.: 'Cavitation bubble behavior and bubble-shock wave interaction near a gelatin surface as a study of in vivo bubble dynamics', Applied Physics B: Lasers and Optics, 2000, 70, (1), pp. 139-149

[3] Qin, S., and Ferrara, K.W.: 'Acoustic response of compliable microvessels containing ultrasound contrast agents', Phys Med Biol, 2006, 51, (20), pp. 5065-5088

[4] Hynynen, K., McDannold, N., Vykhodtseva, N., and Jolesz, F.A.: 'Noninvasive MR imaging-guided focal opening of the blood-brain barrier in rabbits', Radiology, 2001, 220, (3), pp. 640-646

[5] Hynynen, K., McDannold, N., Vykhodtseva, N., Raymond, S., Weissleder, R., Jolesz, F.A., and Sheikov, N.: 'Focal disruption of the blood-brain barrier due to 260-kHz ultrasound bursts: a method for molecular imaging and targeted drug delivery', J Neurosurg, 2006, 105, (3), pp. 445-454

[6] Sheikov, N., McDannold, N., Vykhodtseva, N., Jolesz, F., and Hynynen, K.: 'Cellular mechanisms of the blood-brain barrier opening induced by ultrasound in presence of microbubbles', Ultrasound Med Biol, 2004, 30, (7), pp. 979-989

[7] Chen, S., Ding, J.H., Bekeredjian, R., Yang, B.Z., Shohet, R.V., Johnston, S.A., Hohmeier, H.E., Newgard, C.B., and Grayburn, P.A.: 'Efficient gene delivery to pancreatic islets with ultrasonic microbubble destruction technology', Proc Natl Acad Sci U S A, 2006, 103, (22), pp. 8469-8474

[8] Choi, J.J., Pernot, M., Brown, T.R., Small, S.A., and Konofagou, E.E.: 'Spatio-temporal analysis of molecular delivery through the blood-brain barrier using focused ultrasound', Phys Med Biol, 2007, 52, (18), pp. 5509-5530

[9] Miller, D.L., Averkiou, M.A., Brayman, A.A., Everbach, E.C., Holland, C.K., Wible, J.H., Jr., and Wu, J.: 'Bioeffects considerations for diagnostic ultrasound contrast agents', J Ultrasound Med, 2008, 27, (4), pp. 611-632

[10] McDannold, N., Vykhodtseva, N., and Hynynen, K.: 'Effects of Acoustic Parameters and Ultrasound Contrast Agent Dose on Focused-Ultrasound Induced Blood-Brain Barrier Disruption', Ultrasound Med Biol, 2008, 20, pp. 20

[11] Borden, M.A., Kruse, D.E., Caskey, C.F., Zhao, S., Dayton, P.A., and Ferrara, K.W.: 'Influence of lipid shell physicochemical properties on ultrasound-induced microbubble destruction', IEEE Trans Ultrason Ferroelectr Freq Control, 2005, 52, (11), pp. 1992-2002

[12] Caskey, C.F., Qin, S., Dayton, P., and Ferrara, K.: 'Microbubble tunneling in gel phantoms', JASA Express Letters, 2009, at press

[13] Dayton, P.A., Allen, J.S., and Ferrara, K.W.: 'The magnitude of radiation force on ultrasound contrast agents', J Acoust Soc Am, 2002, 112, (5 Pt 1), pp. 2183-2192

[14] Dayton, P.A., Morgan, K. E., Klibanov, A. L. S., Brandenburger, G., Nightingale, K. R., and Ferrara, K. W. : 'A preliminary evaluation of the effects of primary and secondary radiation forces on acoustic contrast agents', Trans. Ultrason. Ferroelectr. Freq. Control 1997, 44, pp. 1264–1277.